Journal of Materials Chemistry B

Accepted Manuscript

ROYAL SOCIETY OF CHEMISTRY

www.rsc.org/materialsB

Cite this: DOI: 10.1039/c0xx00000x

www.rsc.org/xxxxxx

ARTICLE TYPE

Aggregation inhibition for graphene oxide nanosheets in polyelectrolyte solutions and the assembly of nanocapsules with graphene oxide nanosheets as template†

Jing Xin[a], Renjie Zhang*[ab], Wanguo Hou[a]

Received (in XXX, XXX) Xth XXXXXXXXX 20XX, Accepted Xth XXXXXXXXX 20XX
DOI: 10.1039/b000000x

A strategy of inhibiting aggregation of graphene oxide (GO) nanosheets is proposed in this work, which is important to understand the physical chemistry on the stability of GO and the related factors. First, GO nanosheets (1.5 - 2.5 μm wide and 1.0 nm thick) were prepared by a modified Hummers' method. Then layer-by-layer (LbL) self-assembly of polyelectrolytes on GO nanosheets was carried out to get nanocapsules, whose premise is the aggregation inhibition of GO based on Debye-Hückel theory by considering the polyelectrolyte chain length and salt concentration. Low molecular weight polyelectrolytes and 0.5 mol·L^{-1} NaCl solution were proved to be essential to inhibit the aggregation of GO nanosheets. On the basis of the aggregation inhibition, GO loading a hydrophobic drug, paclitaxel (PTX) were encapsulated by polyelectrolytes, showing a high loading capability of 0.4 mg·mg^{-1} and good dispersion stability. By assembling gold nanoparticles (AuNPs) in the shell, the PTX released fast from these nanocapsules under near infrared (NIR) irradiation. The strategy of successful aggregation inhibition of GO nanosheets in polyelectrolyte matrix, as well as the stable loading and controlled fast release of hydrophobic drugs, paves new paths for GO-based advanced nanomaterials and pharmaceutics.

Introduction

Graphene has been a research hotspot due to the physicochemical properties and vast applications.[1-4] Graphene oxide (GO) nanosheets have been studied extensively as carriers of hydrophobic molecules such as anti-cancer drugs.[5-6] Pure hydrophobic drugs do not disperse but form aggregates in aqueous solution. Carriers should be found to load and deliver drugs. GO is one of the best candidates due to its surfactant-like amphiphilic property. On one hand, the oxidized groups like -COOH enable the good solubility of GO-loaded drugs in aqueous solution; on the other hand, the hydrophobic sp^2 domains on the GO surface load the drugs. However, between these drugs and GO, there are strong π-π stacking interaction and hydrogen bonds. As a result, the drugs on GO can hardly release.[7-8] Only low pH (2.0) is reported to decrease the interaction and stimulate their release.[9] However, such low pH is much lower than the pH (5.6 - 7.6 [10]) of cancer cells.

To make the GO family applicable in more functional systems, layer-by-layer (LbL) self-assemblies on the molecular level is a good candidate.[11-12] In the LbL capsules, functional molecules can be encapsulated either in core or in shell, and show priority control release by stimulus of internal change of salt concentration or external light irradiation. Near infrared (NIR) light responsive capsules can deliver drugs to targeted sites, where drugs release fast to cancer cells without damage to normal tissues or cells after remote light stimulus.[13] This is of great importance for biomedical applications.[14]

GO nanosheets have recently been assembled in the shell of spherical microcapsules.[15-16] But GO nanosheets have not been reported to serve as template of nanocapsules in the shape of nanosheet. Such GO-based nanocapsules with a big aspect ratio of lateral dimension to thickness should be superior to the microcapsules concerning transmembrane drug delivery.

It is a big challenge to use GO nanosheets as template for nanocapsules. Because during the assembly process nanoparticles like GO tend to be bridge-linked to aggregates by the shell component, polyelectrolyte macromolecules.[17]

In this paper, we proposed a strategy of inhibiting aggregation of GO nanosheets by applying the Debye-Hückel theory, where the polyelectrolyte molecular weight and salt concentration, as well as the net charges and flexibility of polyelectrolytes are considered. Then GO nanosheets are successfully employed as template to obtain nanocapsules coated with polyelectrolytes. The strategy of aggregation inhibition of GO is also proved by loading a hydrophobic drug, paclitaxel (PTX) on GO, which is denoted by GO+PTX. Deposition of polyelectrolytes on the GO+PTX nanosheets as template also produces well-dispersed nanocapsules. These nanocapsules exhibit interesting fast release of PTX under remote control of NIR irradiation.

The novel strategy of inhibition of GO aggregates in polyelectrolyte solution and the assembly of nanocapsules with GO as template should enrich the physical chemistry and the

family of GO-based nanomaterials.

Experimental

Materials

Graphite powder (99.9995%) with an average lateral dimension of 2-14 μm was purchased from Alfa Aesar (U.S.A.). The poly (allylamine hydrochloride) (PAH, M.W.=15, 58 and 70 kDa) and poly (sodium 4-styrenesulfonate) (PSS, M.W.=70 kDa) were purchased from Sigma-Aldrich Inc. (Germany). All commercial polyelectrolytes were used without further purification. PTX (> 99.0% purity) was purchased from Beijing Huafeng United Technology Co., Ltd. Chloroauric acid tetrahydrate ($HAuCl_4 \cdot 4H_2O$), trisodium citrate dihydrate, methanol, dichloromethane (DCM), $KMnO_4$ and NaCl were analytical reagents. Dialysis tubings with a molecular weight cutoff of 14 kDa were purchased from Beijing Jingke Hongda Co., Ltd. Pure water with a specific resistivity of 18.2 MΩ·cm at 25 ºC was used in all experiments.

Preparation of GO.

GO was prepared using a modified Hummers' method.[18-19] Briefly, using a ball mill, a mixture of 1.0 g graphite powder and 50.0 g NaCl was milled for 2 h by 357.0 g stainless steel balls (64 balls of 8 mm in diameter and 101 balls of 5 mm in diameter). The graphite flakes were air dried after washing to remove NaCl and then added to 23.0 mL of concentrated H_2SO_4, kept stirring for 12 h at 0 ºC. Then 6.0 g $KMnO_4$ was added while keeping the temperature below 20 ºC. The mixture was stirred at 40 ºC for 30 min and then stirred at 90 ºC for 90 min. 46.0 mL of water was added and the mixture was stirred at 105 ºC in an oil-bath for 25 min. Subsequently, 140.0 mL of water and 10.0 mL of 30% H_2O_2 solution were added to terminate the reaction. The color of the mixture solution was yellow. The GO nanosheets in the mixture were thoroughly washed with water and centrifuged until the pH value does not change any longer, corresponding to a pH value of 5.5. Finally, the GO suspension in water was sonicated at 1.2 kW for 1 hour to be further exfoliated.

Assembly of GO/(PAH/PSS)$_4$ nanocapsules.

GO nanosheets in water suspension (1.6 mg·mL^{-1}, 1.0 mL) were used as template to assemble nanocapsules. These nanocapsules were assembled by alternating adsorption of polyelectrolytes of PAH and PSS. Each adsorption cycle (15 min incubation under shaking) was completed by centrifugation and washing. After the last centrifugation, 0.5 mL of water was added and sonicated for 10 s to disperse the pellets against aggregation, facilitating the adsorption of next layer of polyelectrolyte.

Preparation of AuNPs.

According to Frens' method,[20] 50.0 mL of chloroauric acid (0.01 wt%) was heated to boiling under stirring, followed by pouring 0.5 mL of trisodium citrate solution (1.0 wt%). The mixture was heated to boiling, turning violet within 1 - 3 min.

Preparation of GO nanosheets loading PTX (denoted by GO+PTX).

The GO+PTX nanosheets were obtained by referring to literature methods,[21-22] 3.6 mL of 2.3×10^{-3} mol·L^{-1} PTX in methanol was added dropwise to 4.5 mL of 1.6 mg·mL^{-1} GO suspension in water under rapid stirring. The mixture was stirred for 30 min, sonicated for 30 min and stirred for 30 min. Concentrated to 4.5 mL by rotary evaporation, the mixture was dialyzed against water for 48 h to remove free PTX molecules, followed by filtration to remove large PTX particles. The loading amount of PTX on GO was calculated by using 2.0 mL of DCM to extract 50 μL GO+PTX suspension. The loading capability of PTX was determined by UV spectra based on a working curve. The working curve of absorbance was acquired by plotting the absorbance of PTX in DCM at 232 nm at the concentration of $2.3\times10^{-7} - 2.3\times10^{-5}$ mol·L^{-1}.

Preparation of (GO+PTX)/(PAH/AuNPs)/(PAH/PSS)/PAH nanocapsules.

GO+PTX nanosheets suspended in 1.0 mL of water were used as template. The nanocapsules were assembled by alternating adsorption of PAH, AuNPs, PAH, PSS and PAH. Each adsorption cycle included 15 min incubation in polyelectrolytes solutions or 30 min in AuNPs solutions, washing followed by centrifugation. After the last centrifugation, 0.5 mL of water was added and sonicated for 10 s.

Release profiles of PTX from (GO+PTX)/(PAH/AuNPs), (GO+PTX)/(PAH/AuNPs)/(PAH/PSS) and (GO+PTX)/(PAH/AuNPs)/(PAH/PSS)/PAH nanocapsules under NIR irradiation.

In a typical procedure, 0.2 mL of (GO+PTX)/(PAH/AuNPs) suspension was put in a dialysis tubing immersed in 10.0 mL of phosphate buffered saline (PBS) (pH=7.4) solution under NIR lamp with a cutoff filter of 800 nm (irradiation intensity, 40 mW·cm^{-2}) and stirring. At each predetermined time interval, the tubing was moved to another 10.0 mL of fresh PBS (pH=7.4) solution under the same conditions. Then 3.0 mL of DCM was used to extract the released PTX into the PBS solution. The PTX amount released into PBS solution was quantitatively determined by UV spectra on the basis of a working curve.

The release profiles of PTX from other nanocapsules into PBS solution were measured following the procedure described above.

Characterization.

UV-Vis absorption spectra of GO-templated nanocapsules were recorded with quartz cells on a HP-8453 diode array spectrophotometer (Agilent, U.S.A.) with a resolution of 2 nm. FTIR spectra of nanocapsules were recorded by a VERTEX-70 FTIR spectrometer (Bruker, Germany). The average size and zeta potentials of GO-templated nanocapsules were measured using Zetasizer Nano-ZS90 (Malvern Instrument Ltd., U.K.) in dilute solutions at room temperature.[39] Scanning electron microscopy (SEM) measurement was carried out on a JSM-6700F (Jeol, Japan) instrument at an operation voltage of 3 keV. The SEM samples were prepared by dropping 5 μL of GO nanosheets or nanocapsule suspensions onto a silicon substrate with low specific resistivity of 0.011-0.012 Ω·cm and air dried, then sputtered with platinum. Transmission electron microscopy (TEM) images of GO were obtained with JEM-1011 (Jeol, Japan) under an accelerating voltage of 100 kV. The TEM samples were prepared by dropping 5 μL of GO onto copper grids covered with holey carbon-supported films. GO and nanocapsules were both

observed by atomic force microscopy (AFM) with Nanoscope IIIA (Digital Instrument, U.S.A.) in tapping mode. X-ray photoelectron spectroscopy (XPS) was carried out on Phi 5300 ESCA system (Perkin-Elmer, U.S.A.) with Mg (Kα) irradiation (photoelectron energy 1253.6 eV). The analysis spot area was 1.0×3.5 mm^2. The XPS samples were prepared by dropping 10 μL GO suspension onto a silicon substrate followed by air drying. The procedure was repeated for 5 times. Powder X-ray diffraction (XRD) for GO nanosheets was performed using D8 ADVANCE X-ray diffractrometer (Bruker, Germany) operated at 40 mA and 40 kV with Cu (Kα) radiation.

Results and discussions

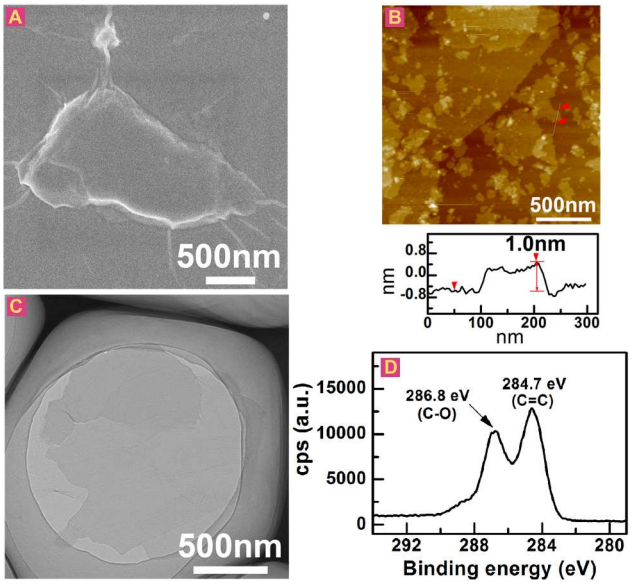

Fig. 1 (A) SEM micrograph of a GO nanosheet. (B) AFM height image and section analysis of GO nanosheets, (C) TEM micrograph of a GO nanosheet. (D) C1s XPS spectrum of GO nanosheets

Two steps were added as modification of the Hummers' method to prepare small sized GO nanosheets with a single layer of carbon atom lattice. 1) Before the chemical oxidization, graphite powder and NaCl were mixed and milled to make the particles of graphite powder smaller; 2) After the oxidization reaction, the GO suspension in water was sonicated at a high power (1.2 kW) to fully exfoliate GO nanosheets. SEM, AFM and TEM images (Fig. 1A - C) show the morphological information of the GO nanosheets. They have a lateral dimension of 1.5 - 2.5 μm and a thickness of 1.0 nm. Typically, the thickness of GO with a single layer of the carbon atom lattice is 0.7 - 1.0 nm.[23] So we obtained a single layer of GO nanosheets. The XRD pattern (Fig. S1 in the ESI) exhibits a typical sharp peak at 12.2° (2θ) with a periodic interlayer spacing of 0.7 nm, consistent with a single layer of GO, the same as what observed by others.[24] C1s XPS (Fig. 1D) shows two different existence states of carbon atoms on GO: the oxygenated carbon in the C-O group (286.8 eV) and the sp^2 C=C carbon (284.7 eV).[25]

The oxygenated carbons of GO nanosheets enable the good dispersion in water, which is necessary for the LbL assembly of nanocapsules. The zeta potential of GO nanosheets is -39.9 mV at pH=5.5, showing that negative charges are on GO. The zeta potential of GO is dependent on pH and degrees of oxidation. At pH=10, the zeta potential of GO has been reported to be about -50 and -45 mV by Kim et al.[26] and Chen et al.,[27] respectively. The difference should be due to different degrees of oxidation. The zeta potential increases from about 31 to 51 mV for GO by increasing the oxidation level.[28] Our GO nanosheets show good stability, dispersing very well in water after 2 years. Driven by electrostatic interaction, GO should be capable of being assembled in capsules either as template or as shell component.

GO nanosheets have recently been assembled in the shell of spherical microcapsules.[15-16] However, using GO as core template is a big challenge for the deposition of polyelectrolytes in the LbL assembly. Because during the assembly process nanoparticles tend to be bridge-linked to aggregates by the shell component, polyelectrolyte macromolecules.[17] A solution to this challenge should be found to assemble nanocapsules, which should be superior for transmembrane drug delivery.

GO nanosheets carry negative charges, so a positively charged polyelectrolyte should be used for the deposition as the first layer on GO. Commercial PAH with different molecular weight is used as model polyelectrolytes. The PAH with the most commonly used molecular weight of 70 kDa[29-30] was first tried. However, when 3.0 mL of PAH solution was added in 1.0 mL of clear transparent GO suspension, the suspension became immediately cloudy and a large number of flocculent precipitates appeared (Fig. 2A). Changing the PAH from the molecular weight of 70 kDa to 58 kDa, flocculent precipitates still appeared. Changing to PAH of 15 kDa, the suspension was clear transparent without flocculent precipitates (Fig. 2B). Therefore, the selection of low molecular weight PAH of 15 kDa rather than the mostly used PAH of 70 kDa is the strategy we proposed in this work to inhibit the aggregation of GO nanosheets.

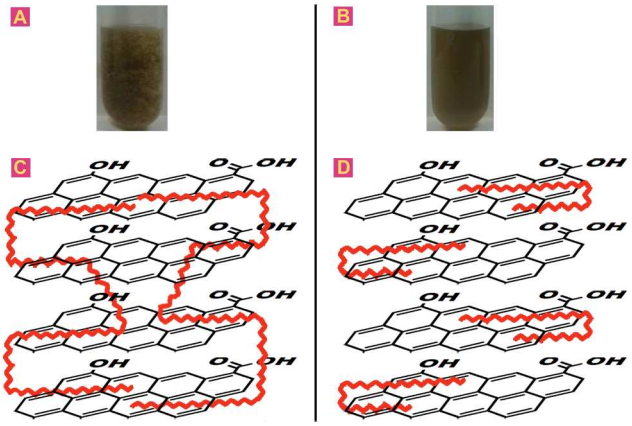

Fig. 2 (A) GO aggregates in PAH with the mostly used molecular weight of 70 kDa or that of 58 kDa. (B) Transparent GO suspension in PAH with low molecular weight of 15 kDa. Schematic illustration of (C) bridge-linking and (D) aggregation inhibition effect of PAH for GO by using long and short molecular weight of PAH, respectively. 0.5 $mol \cdot L^{-1}$ NaCl is used for both cases.

The above PAH and GO solutions both contained 0.5 $mol \cdot L^{-1}$ NaCl, an optimum concentration in the range of 0.2 - 1.0 $mol \cdot L^{-1}$. More concentrated NaCl than 0.5 $mol \cdot L^{-1}$ induced aggregation for both the GO nanosheets suspension and the polyelectrolyte solutions. On the contrary, in more diluted NaCl solutions of less than 0.5 $mol \cdot L^{-1}$, the addition of PAH in GO suspension resulted in flocculent precipitates.

It is necessary to discuss the effect of the molecular weight of PAH and the concentration of NaCl on the aggregation of GO nanosheets. It has been shown that aggregation tends to take place between charged spherical microparticles and polyelectrolytes.[17] Our work shows that extremely good care should be taken when mixing GO nanosheets with polyelectrolytes. The mostly used PAH of 70 kDa deposits well on the spherical particles of several micrometers in diameters.[30] However, it does not work for the GO of 1.5 - 2.5 μm wide and 1.0 nm thick. Only when the PAH with low molecular weight of 15 kDa in 0.5 mol·L^{-1} NaCl is used, can these GO nanosheets be well coated without aggregation. To explain these results, two parameters (flexibility and length of molecular chains) should be referred. The inverse Debye-Hückel screening length κ is involved,

$$\kappa = \sqrt{8\pi l_b c}\ (nm^{-1})$$

where l_b is the Bjerrum length, and c is the ionic strength of an added monovalent salt (mol·L^{-1}).[31-32] The added salt reduces the Debye-Hückel screening length κ^{-1}, so concentrated NaCl larger than 0.5 mol·L^{-1} induces both the charged GO nanosheets and the PAH molecules to aggregation. On the contrary, an appropriate concentration of NaCl reduces to some extent the net charges carried by the PAH, so decreases the stiffness of the PAH due to less like-charge repulsion and increases the flexibility of polyelectrolyte chains, facilitating the deposition of PAH on GO. The increased flexibility also induces the conformation change of PAH from extended to coiled. The end-to-end distance of PAH decreases, which is favourable for the deposition of PAH on GO nanosheets against bridge-linking in the direction of thickness of GO. Too diluted NaCl does not decrease obviously the flexibility of the polyelectrolyte. So an appropriate concentration of NaCl should be used, which is optimized to be 0.5 mol·L^{-1}. Although salt concentration has the same effect on PAH, regardless of molecular weight, the PAH with the mostly used molecular weight of 70 kDa has too long a molecular chain compared to the thickness of GO, even when the coiled conformation of PAH is adopted at the NaCl concentration of 0.5 mol·L^{-1}. In summary, lower molecular weight of PAH having short end-to-end distance should be used; simultaneously salt at an appropriate concentration should be used to increase the molecular flexibility of PAH.

Based on the above discussion and our experimental results, the effect of high and low molecular weight of PAH on GO in 0.5 mol·L^{-1} NaCl is schematically illustrated in Fig. 2C-D. Low molecular weight PAH of 15 kDa is shorter and flexible enough to avoid bridge-linking between nearby GO nanosheets, successfully enabling the deposition of PAH on GO. On the contrary, the mostly used PAH of 70 kDa (or that of 58 kDa) has a higher molecular weight with a molecular chain length of about 5 (or 3) times long of that of 15 kDa. The probability of binding nearby GO nanosheets together increases greatly, leading to the formation of flocculent precipitates through bridge-linking especially in the direction of thickness of GO. The C-C bond length in $-CH_2-CH_2-$ is 0.15 nm. Assuming that the PAH molecular chain is fully extended, the average chain lengths of PAH with the molecular weight of 70 kDa and 15 kDa are calculated to be 112 nm and 24 nm, respectively. The fact that the lateral size of GO sheet is much larger than that of the polyelectrolytes is favourable for the homogeneous LbL assembly of polyelectrolytes. As a result, a lot of microcapsules have been obtained by depositing polyelectrolytes on microspheres of several microns in diameter.[29] However, the thickness of GO nanosheets is only 1.0 nm, much smaller than the length of PAH, in addition to the negative charges carrying on the edge of GO, the positively charged PAH bridging for the GO must be effectively inhibited.

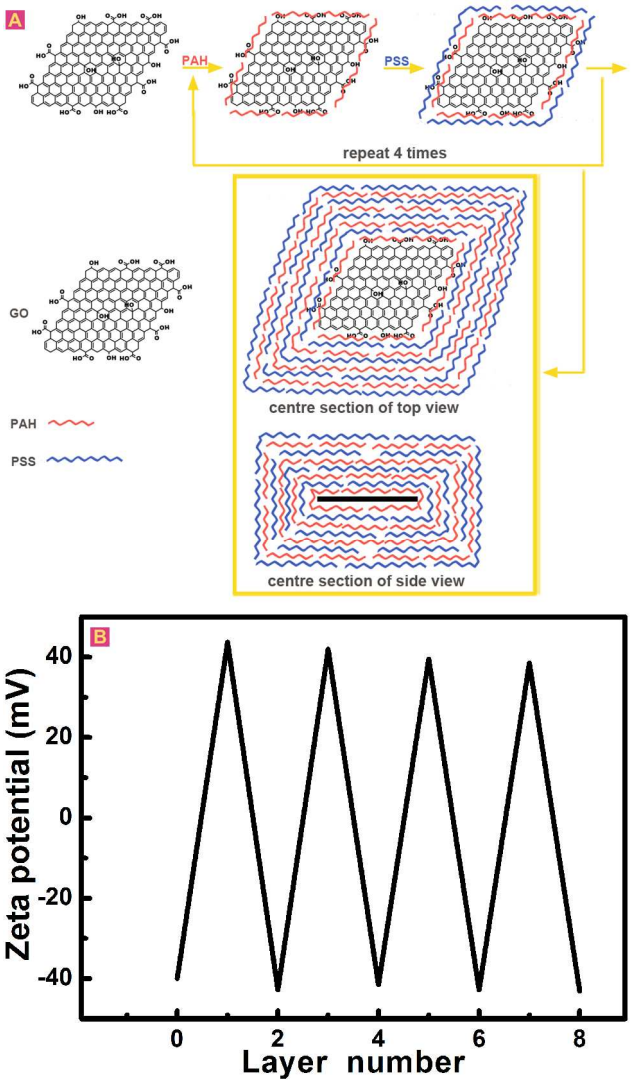

Fig. 3 Assembly of GO nanosheets templated nanocapsules. (A) Schematic illustration of the LbL assembly of PAH and PSS on a GO nanosheet. (B) Zeta potentials during the LbL assembly of PAH and PSS on GO nanosheets; the layer number 0 corresponds to GO nanosheets; the layer numbers 1, 3, 5, 7 correspond to PAH, and the layer numbers 2, 4, 6, 8 correspond to PSS.

As described in a reference[33], GO can be defined as microsheets when one wants to emphasize the micrometer scale of the lateral dimension in cases where it is correlated to properties or behaviours. In our paper, we solve the problem of aggregation of GO in the thickness (of only 1.0 nm per layer) direction by selecting appropriate molecular weight of PAH. Thus it is better to define GO as nanosheets to emphasize the

thickness issue of GO correlated with the stability of GO-polymer composites.

On the basis of the aggregation inhibition, GO nanosheets are used as template to successfully assemble nanocapsules by alternating deposition of lower molecular weight PAH and PSS, which is illustrated in Fig. 3A. Polyelectrolyte molecules bind not only at the edges but also at overall surface of GO to form GO-templated nanocapsules, as shown in the centre section of top view and side view of Fig. 3A. In the UV-Vis spectra of GO/PAH nanocapsules (Fig. S2 in the ESI), an absorption peak at about 230 nm is due to the π-π* electronic transition of the sp^2 carbon atoms of GO.[34] After the PSS layer is assembled, the peak around 230 nm is associated with the π-π* electronic transition of the sp^2 carbon atoms of GO and the π-π* electronic transition of PSS. The absorbance increases with the increase of layer number of PSS, which proves the successful assembly of PSS on GO nanosheets. The zeta potentials (Fig. 3B) change alternatingly during the deposition of each layer, indicating the successful assembly of PAH and PSS on GO nanosheets. The XPS results of GO/$(PAH/PSS)_4$ nanocapsules (Fig. S3 in the ESI) show the presence of N atoms of PAH and S atoms of PSS on GO/$(PAH/PSS)_4$, confirming the successful assembly of PAH and PSS on GO nanosheets.[35-36] The pure PAH has characteristic peaks ν_{N-H} (3451 cm^{-1}), δ_{N-H} (1625 cm^{-1}) and δ_{C-H} (1384 cm^{-1}).[37] The pure PSS has characteristic peaks of O-H (3439 cm^{-1}), CH peaks (2924, 2853 cm^{-1}), SO_3^- peaks (1415, 1040 cm^{-1}), ν_{C-C} (1632, 1445 cm^{-1}) and δ_{C-H} (1121, 1384 cm^{-1}).[36] The FTIR spectra of GO/$(PAH/PSS)_4$ nanocapsules (Fig. S4 in the ESI) show main peaks of PAH and PSS, including the ν_{N-H} (3441 cm^{-1}) of PAH and the SO_3^- (1415, 1036 cm^{-1}) of PSS, indicating the successful assembly of PAH and PSS on GO nanosheets.

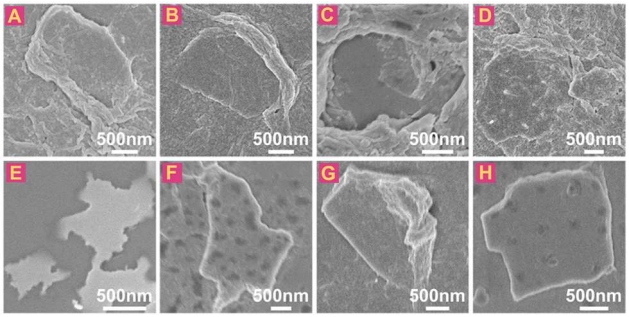

Fig. 4 SEM micrographs of GO-templated nanocapsules of (A) GO/PAH, (B) GO/(PAH/PSS), (C) GO/(PAH/PSS)/PAH, (D) GO/$(PAH/PSS)_2$, (E) GO/$(PAH/PSS)_2$/PAH, (F) GO/$(PAH/PSS)_3$, (G) GO/$(PAH/PSS)_3$/PAH and (H) GO/$(PAH/PSS)_4$.

SEM images of nanocapsules (Fig. 4A - H) show that the lateral dimension of the GO-templated nanocapsules is 1.0 - 2.5 μm. The nanocapsules remain the profile of nanosheets with the stepwise deposition of polyelectrolytes. The thickness of the nanocapsules increases gradually with the increasing layer number, as shown by the section analysis of the AFM height images (Fig. 5A - H). For example, the thickness values of GO/PAH, GO/(PAH/PSS) and GO/$(PAH/PSS)_4$ nanocapsules are 2.5 , 4.7 and 16.1 nm, respectively. The single layer thickness of PAH or PSS is calculated to be 0.9 nm by deducing the thickness of GO from the thickness of GO/$(PAH/PSS)_4$ nanocapsules and assuming an equal thickness of each polyelectrolyte layer, that is, (16.1-1.0)/(8×2) = 0.9 nm. The gradually increased thickness of nanocapsules also proves the successful assembly of the PAH and PSS on the GO nanosheets.

During the LbL assembly, the nanocapsules were subject to continous shaking and more than ten times of centrifugation at 16000 rpm (21752 *g*). The nanocapsules are collected at the bottom of centrifuge tube instead of at the suspension. GO nanoplates themselves are not flat, showing many folds and creases after repeated centrifugation. It is easy to understand that the surface of the nanocapsules is not flat, as shown in the AFM images of GO-templated nanocapsules.

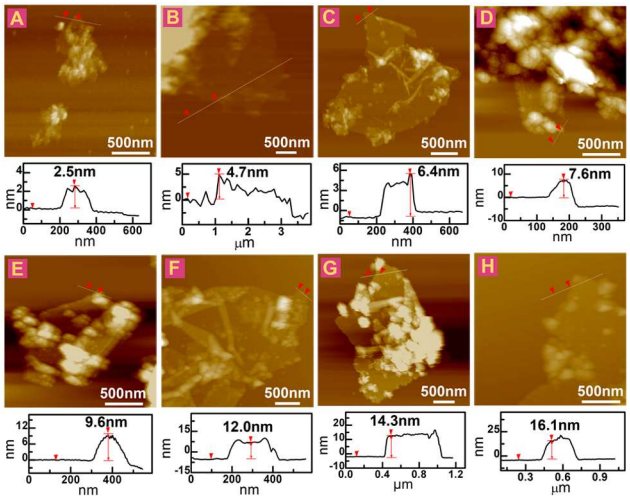

Fig. 5 AFM height images and section analysis of GO-templated nanocapsules of (A) GO/PAH, (B) GO/(PAH/PSS), (C) GO/(PAH/PSS)/PAH, (D) GO/$(PAH/PSS)_2$, (E) GO/$(PAH/PSS)_2$/PAH, (F) GO/$(PAH/PSS)_3$, (G) GO/$(PAH/PSS)_3$/PAH, and (H) GO/$(PAH/PSS)_4$.

It is difficult to determine that the whole surface is covered by polymers to form nanocapsules. Due to the GO thickness of only about 1.0 nm, GO-based nanocapsules appear as nanosheets. However, the polyelectrolytes adsorb not only on the surface but also at edge of GO sheets. Because the hydrophobic interaction (between the molecular main chain of the polyelectrolytes and the homogenous and random sp^2 domains on GO surface) and electrostatic interaction (between the negatively charged GO and positively charged PAH) should be driving forces for the homogenous distribution of PAH on the surface of GO. Regarding to electrostatic interaction, charges are mainly carried at the edge of GO.[38]

To evaluate dispersion stability of GO based materials, assuming that the particles are spherical, measurement of average size instead of absolute size of graphene sheets has been proposed.[39] Accordingly, the average hydrodynamic size of the nanocapsules is 600 nm (pH = 7), corresponding to the zeta potential of -43.1 mV. Obviously the average hydrodynamic size is quite different from those shown in the microscopic images. The former can only serve as reference for the dispersion stability. These nanocapsules disperse stably in water after 3 months.

The loading amount of PTX on GO is about 0.4 $mg \cdot mg^{-1}$. The strategy of aggregation inhibition is also proved by loading PTX on GO, which is denoted by GO+PTX. The thickness of the

GO+PTX is 1.3 nm (Fig. S5 in the ESI). Deposition of polyelectrolytes on the GO+PTX nanosheets as template produces stably dispersed nanocapsules in water. Gold nanoparticles (AuNPs) are assembled in the shell to enable the nanocapsules to absorb NIR irradiation.[40] The nanocapsules remain as nanosheets with the lateral dimension of 1.5 - 2.5 μm (Fig. 6A - D), similar to that of the GO template. The thickness values of (GO+PTX)/PAH, (GO+PTX)/(PAH/AuNPs), (GO+PTX)/(PAH/AuNPs)/(PAH/PSS) and (GO+PTX)/(PAH/AuNPs)/(PAH/PSS)/PAH are 2.9, 4.4, 7.3 and 9.3 nm, respectively, as shown by section analysis of the AFM height images (Fig. 6E - H).

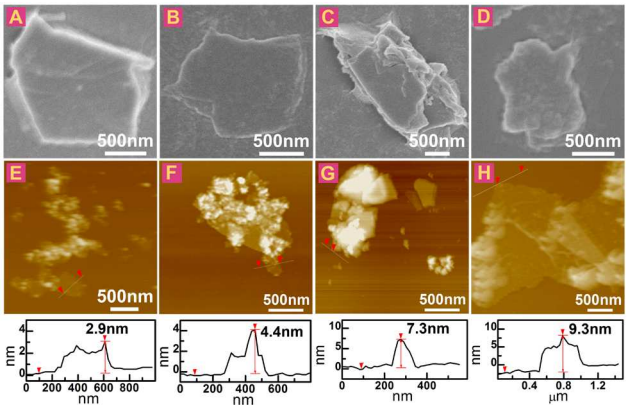

Fig. 6 SEM micrographs of nanocapsules of (A) (GO+PTX)/PAH, (B) (GO+PTX)/(PAH/AuNPs), (C) (GO+PTX)/(PAH/AuNPs)/(PAH/PSS), and (D) (GO+PTX)/(PAH/AuNPs)/(PAH/PSS)/PAH. AFM height images and section analysis of nanocapsules of (E) (GO+PTX)/PAH, (F) (GO+PTX)/(PAH/AuNPs), (G) (GO+PTX)/(PAH/AuNPs)/(PAH/PSS), and (H) (GO+PTX)/(PAH/AuNPs)/(PAH/PSS)/PAH.

PTX did not release from the nanocapsules without AuNPs in the temperature range of 25.0 – 50.0 ºC under NIR irradiation. When AuNPs were assembled in the nanocapsules, PTX released quickly and reached the release balance fast in a mild temperature range of 25.0 ºC to the physiological temperature of about 37.0 ºC under NIR irradiation at neutral pH (Fig. 7). Approximately 70% and 76% of PTX released from the (GO+PTX)/(PAH/AuNPs) and (GO+PTX)/(PAH/AuNPs)/(PAH/PSS) nanocapsules, respectively. The release balance was reached within 150 s. About 87% of PTX releases from the (GO+PTX)/(PAH/AuNPs)/(PAH/PSS)/PAH nanocapsules, and the release balance was reached within 210 s.

Why does not PTX release until 50 ºC without AuNPs, while PTX releases from the nanocapsules with AuNPs under NIR irradiation? The reason should be due to the local temperature effect by AuNPs. AuNPs absorb NIR irradiation and produce local heat. The local temperature (which is difficult to measure) of AuNPs, nearby GO and polyelectrolyte molecules can all be higher than 50.0 ºC, although the measured temperature of the nanocapsules suspension is no more than 40.0 ºC. The local high temperature decreases the interactions of π-π stacking[41] and the hydrogen bonds,[42] enabling the unloading of PTX from GO nanosheets. In addition, the local high temperature also increases permeability of the polyelectrolyte layers,[43] enabling the release of PTX from the nanocapsules.

Regarding to the pH dependence, PTX does not release from GO unless low pH = 2.0 is reached, similar to what reported by Yang and co-workers.[9] So the release stimulated by NIR irradiation at around physiologically neutral pH is practically more important.

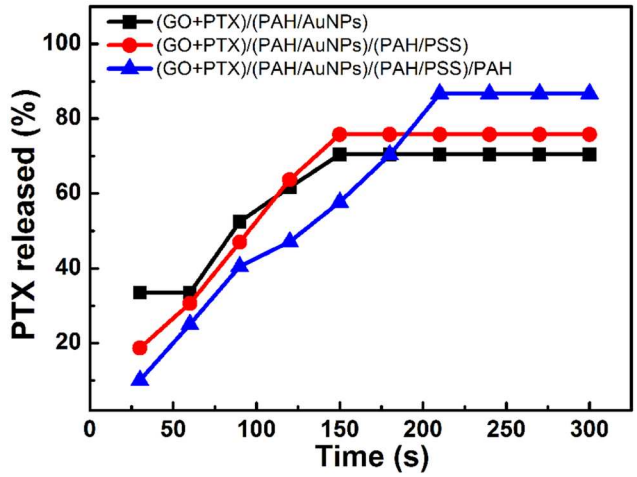

Fig. 7 Release profiles of PTX from nanocapsules containing AuNPs under NIR irradiation at pH=7.4.

Conclusions

The selection of low molecular weight of PAH molecules in 0.5 mol·L^{-1} NaCl proves a successful strategy to inhibit the aggregation of small GO nanosheets. Shorter molecular chain and good chain flexibility are favourable for deposition of PAH on GO against bridge-linking. With this strategy, GO nanosheets as well as GO nanosheets loading a hydrophobic drug, PTX, can be encapsulated by polyelectrolytes to obtain nanocapsules in the shape of nanosheets with good dispersion stability in water. PTX releases fast from nanocapsules containing AuNPs under NIR irradiation. This work not only understands better the physical chemistry of the dispersion stability of GO nanosheets in aqueous solution of polyelectrolytes, but also paves new paths for the development of GO-based advanced nanomaterials and pharmaceutics.

Acknowledgements

This work was supported by the National Nature Science Foundation of China (21273135), Shandong Provincial Natural Science Foundation, China (ZR2010BM039), Independent Innovation Foundation of Shandong University (2011JC026), and the Max Planck Society, Germany. We also thank Prof. Xiyou Li for providing the access to the AFM.

Notes and references

[a] *Key Laboratory of Colloid and Interface Chemistry of the Ministry of Education of the P. R. China*
Shandong University
Jinan 250199
P. R. China.
E-mail: zhrj@sdu.edu.cn; Fax: +86-531-88364464; Tel.: +86-531-88366233
[b] *Key Laboratory of Special Functional Aggregated Materials of the Ministry of Education of the P. R. China*

Shandong University
Jinan 250199
P. R. China.

† Electronic Supplementary Information (ESI) available. See DOI:10.1039/b000000x/

1. K. S. Novoselov, A. K. Geim, S. V. Morozov, D. Jiang, Y. Zhang, S. V. Dubonos, I. V. Grigorieva and A. A. Firsov, *Science*, 2004, **306**, 666-669.
2. W. Choi, I. Lahiri, R. Seelaboyina and Y. S. Kang, *Crit. Rev. Solid State*, 2010, **35**, 52-71.
3. H. Zhang, G. Grüner and Y. Zhao, *J. Mater. Chem. B*, 2013, **1**, 2542-2567.
4. Y. Wang, H. Chang, H. Wu and H. Liu, *J. Mater. Chem. B*, 2013, **1**, 3521-3534.
5. S. Zhang, M. Zeng, W. Xu, J. Li, J. Li, J. Xu and X. Wang, *Dalton. Trans.*, 2013, **42**, 7854-7858.
6. Z. Wang, C. Zhou, J. Xia, B. Via, Y. Xia, F. Zhang, Y. Li and L. Xia, *Colloids Surf. B*, 2013, **106**, 60-65.
7. D. Depan, J. Shah and R. D. K. Misra, *Mater. Sci. Eng. C*, 2011, **31**, 1305-1312.
8. X. Yang, Y. Wang, X. Huang, Y. Ma, Y. Huang, R. Yang, H. Duan and Y. Chen, *J. Mater. Chem.*, 2011, **21**, 3448-3454.
9. X. Yang, X. Zhang, Z. Liu, Y. Ma, Y. Huang and Y. Chen, *J. Phys. Chem. C*, 2008, **112**, 17554-17558.
10. J. Griffiths, *Brit. J. Cancer*, 1991, **64**, 425-427.
11. C. S. Peyratout and L. Dahne, *Angew. Chem. Int. Ed.*, 2004, **43**, 3762-3783.
12. W. Tong and C. Gao, *J. Mater. Chem.*, 2008, **18**, 3799-3812.
13. D. Volodkin, A. Skirtach and H. Möhwald, *Polym. Int.*, 2012, **61**, 673-679.
14. A. G. Skirtach, C. Dejugnat, D. Braun, A. S. Susha, A. L. Rogach, W. J. Parak, H. Möhwald and G. B. Sukhorukov, *Nano Lett.*, 2005, **5**, 1371-1377.
15. R. Kurapati and A. M. Raichur, *Chem. Commun.*, 2012, **48**, 6013-6015.
16. R. Kurapati and A. M. Raichur, *Chem. Commun.*, 2013, **49**, 734-736.
17. R. Podgornik and M. Licer, *Curr. Opin. Colloid Interface Sci.*, 2006, **11**, 273-279.
18. Z. Liu, J. T. Robinson, X. Sun and H. Dai, *J. Am. Chem. Soc.*, 2008, **130**, 10876-10877.
19. W. S. Hummers Jr and R. E. Offeman, *J. Am. Chem. Soc.*, 1958, **80**, 1339.
20. G. Frens, *Nature (Physical Science)*, 1973, **241**, 20-22.
21. J. M. Berlin, A. D. Leonard, T. T. Pham, D. Sano, D. C. Marcano, S. Yan, S. Fiorentino, Z. L. Milas, D. V. Kosynkin, B. K. Price, R. M. Lucente-Schultz, X. Wen, M. G. Raso, S. L. Craig, H. T. Tran, J. N. Myers and J. M. Tour, *ACS Nano*, 2010, **4**, 4621-4636.
22. C. L. Lay, H. Q. Liu, H. R. Tan and Y. Liu, *Nanotechnology*, 2010, **21**, 065101.
23. D. C. Marcano, D. V. Kosynkin, J. M. Berlin, A. Sinitskii, Z. Sun, A. Slesarev, L. B. Alemany, W. Lu and J. M. Tour, *ACS Nano*, 2010, **4**, 4806-4814.
24. Y. Xu, H. Bai, G. Lu, C. Li and G. Shi, *J. Am. Chem. Soc.*, 2008, **130**, 5856-5857.
25. D. R. Dreyer, S. Park, C. W. Bielawski and R. S. Ruoff, *Chem. Soc. Rev.*, 2010, **39**, 228-240.
26. J. Kim, L. J. Cote, F. Kim, W. Yuan, K. R. Shull and J. Huang, *J. Am. Chem. Soc.*, 2010, **132**, 8180-8186.
27. J. T. Chen, Y. J. Fu, Q. F. An, S. C. Lo, S. H. Huang, W. S. Hung, C. C. Hu, K. R. Lee and J. Y. Lai, *Nanoscale*, 2013, **5**, 9081-9088.
28. K. Krishnamoorthy, M. Veerapandian, K. Yun and S. J. Kim, *Carbon*, 2013, **53**, 38-49.
29. E. Donath, G. B. Sukhorukov, F. Caruso, S. A. Davis and H. Möhwald, *Angew. Chem. Int. Ed.*, 1998, **37**, 2202-2205.
30. R. Zhang, D. Lu, Z. Lin, L. Li, W. Jin and H. Möhwald, *J. Mater. Chem.*, 2009, **19**, 1458-1463.
31. K. K. Kunze and R. R. Netz, *Phys. Rev. Lett.*, 2000, **85**, 4389-4392.
32. R. R. Netz and J. F. Joanny, *Macromolecules*, 1999, **32**, 9026-9040.
33. A. Bianco, H. M. Cheng, T. Enoki, Y. Gogotsi, R. H. Hurt, N. Koratkar, T. Kyotani, M. Monthioux, C. R. Park, J. M. D. Tascon and J. Zhang, *Carbon*, 2013, **65**, 1-6.
34. J. I. Paredes, S. Villar-Rodil, A. Martínez-Alonso and J. M. D. Tascón, *Langmuir*, 2008, **24**, 10560-10564.
35. J. Landoulsi, S. Demoustier-Champagne and C. Dupont-Gillain, *Soft Matter*, 2011, **7**, 3337-3347.
36. H.-K. Jeong, M. H. Jin, K. H. An and Y. H. Lee, *J. Phys. Chem. C*, 2009, **113**, 13060-13064.
37. V. Zucolotto, M. Ferreira, M. R. Cordeiro, C. J. L. Constantino, D. T. Balogh, A. R. Zanatta, W. C. Moreira and O. N. Oliveira, *J. Phys. Chem. B*, 2003, **107**, 3733-3737.
38. L. J. Cote, F. Kim and J. Huang, *J. Am. Chem. Soc.*, 2009, **131**, 1043-1049.
39. D. Li, M. B. Mueller, S. Gilje, R. B. Kaner and G. G. Wallace, *Nat. Nanotechnol.*, 2008, **3**, 101-105.
40. A. S. Angelatos, B. Radt and F. Caruso, *J. Phys. Chem. B*, 2005, **109**, 3071-3076.
41. D. A. Stone, L. Hsu and S. I. Stupp, *Soft Matter*, 2009, **5**, 1990-1993.
42. A. Cooper, *Biophys. Chem.*, 2000, **85**, 25-39.
43. A. G. Skirtach, P. Karageorgiev, M. F. Bédard, G. B. Sukhorukov and H. Möhwald, *J. Am. Chem. Soc.*, 2008, **130**, 11572-11573.